Journal of Coordination Chemistry

ISSN: 0095-8972 (Print) 1029-0389 (Online) Journal homepage: http://www.tandfonline.com/loi/gcoo20

Synthesis and characterization of chiral ruthenium(II) complexes Λ/Δ-[Ru(bpy)$_2$(H$_2$iip)](ClO$_4$)$_2$ as stabilizers of c-myc G-quadruplex DNA

Zhao Zhang, Wenjie Mei, Xiaohui Wu, Xicheng Wang, Baoguo Wang & Sidong Chen

To cite this article: Zhao Zhang, Wenjie Mei, Xiaohui Wu, Xicheng Wang, Baoguo Wang & Sidong Chen (2015) Synthesis and characterization of chiral ruthenium(II) complexes Λ/Δ-[Ru(bpy)$_2$(H$_2$iip)](ClO$_4$)$_2$ as stabilizers of c-myc G-quadruplex DNA, Journal of Coordination Chemistry, 68:8, 1465-1475, DOI: 10.1080/00958972.2015.1014352

To link to this article: http://dx.doi.org/10.1080/00958972.2015.1014352

Journal of Coordination Chemistry, 2015
Vol. 68, No. 8, 1465–1475, http://dx.doi.org/10.1080/00958972.2015.1014352

Synthesis and characterization of chiral ruthenium(II) complexes Λ/Δ-[Ru(bpy)$_2$(H$_2$iip)](ClO$_4$)$_2$ as stabilizers of *c-myc* G-quadruplex DNA

ZHAO ZHANG†, WENJIE MEI*†, XIAOHUI WU†, XICHENG WANG‡, BAOGUO WANG*§ and SIDONG CHEN§

†College of Pharmacy, Guangdong Pharmaceutical University, Guangzhou, PR China
‡The First Affiliated Hospital of Guangdong Pharmaceutical University, Guangzhou, PR China
§College of Public Health, Guangdong Pharmaceutical University, Guangzhou, PR China

(*Received 19 December 2014; accepted 12 January 2015*)

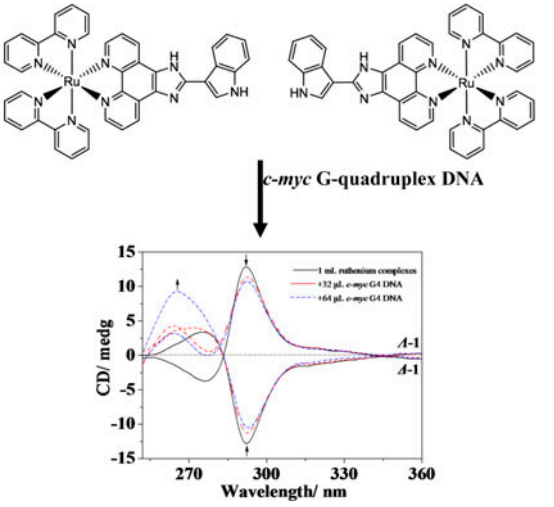

A pair of chiral ruthenium(II) complexes, Λ/Δ-[Ru(bpy)$_2$(H$_2$iip)](ClO$_4$)$_2$, have been synthesized and demonstrated to bind and stabilize *c-myc* G-quadruplex DNA with moderate affinity.

In this article, two chiral ruthenium(II) complexes, **Λ/Δ**-[Ru(bpy)$_2$(H$_2$iip)](ClO$_4$)$_2$ (**Λ-1** and **Δ-1**, bpy = 2,2-bipyridine; H$_2$ii*p* = 2-(indol-3-yl)-imidazo[4,5*f*][1, 10]phenanthroline), were synthesized and investigated as *c-myc* G4 DNA stabilizers. The interaction of both complexes with *c-myc* G4 DNA has been studied using UV–vis spectra, CD spectra, and ITC experiments, and the results show that both isomers strongly bind with *c-myc* G4 DNA. Furthermore, the FRET melting point experiments give a ΔT_m for **Λ-1** and **Δ-1,** which is about 9.5 and 8.3 °C, respectively, indicating that both isomers can stabilize the G-quadruplex conformation of *c-myc* oncogene *in vitro*. As a result, the replication ability of *c-myc* DNA, as evaluated by using PCR-stop assay, by both isomers.

*Corresponding authors. Email: rmgzmwe@live.ucl.ac.uk (W. Mei); gdwangbaoguo@163.com (B. Wang)

Besides, the inhibitory activity evaluated by MTT assay showed that **Λ-1** and **Δ-1** can inhibit the growth of MDA-MB-231 cells, suggesting their potential utility as inhibitors targeting to *c-myc* G-quadruplexe in chemotherapy.

Keywords: Chiral ruthenium(II) complexes; *c-myc* G4 DNA; Stabilizers

1. Introduction

Octahedral ruthenium(II) complexes incorporating imidazole phenanthroline ligands that bind non-covalently with DNA have been extensively investigated for the last 30 years [1–3]. These complexes are used for many purposes, such as anticancer drugs, photosensitizers, and DNA-conformational probes. [4–6]. A number of chiral ruthenium(II) complexes have been designed, and their in vitro antitumor activity, as well as their DNA binding behaviors was evaluated [7, 8]. Chiral ruthenium complexes show high inhibitory activity against various tumor cells [9, 10]. Recently, evidence has shown that ruthenium (II) complexes can also act as potential intercalators of G-quadruplex [11, 12]. For example, ruthenium complex with polypridine has high affinity with G-quadruplex [13]. Thomas *et al.* also indicated that dinuclear ruthenium(II) complexes could bind with G-quadruplex DNA with higher affinities than that with duplex DNA molecules [14]. We have previously demonstrated that ruthenium(II) complexes can induce apoptosis of tumor cells by stabilizing the conformation of *c-myc* G-quadruplex DNA [15].

On the other hand, *c-myc* oncogene, which is overexpressed in various tumors, is linked to several essential intracellular processes of tumor cells, such as proliferation [16] and growth of tumor cells [17], cell-cycle regulation [18] and tumor cell apoptosis [19]. The guanine-rich promoter of *c-myc* oncogene can form a G-quadruplex conformation *via* a Hoogsten hydrogen bond [20, 21]. Compounds, which could stabilize the conformation of *c-myc* G-quadruplex DNA, can downregulate the expression of c-myc, which is closely associated with p53 and Bcl-2 to induce tumor cell apoptosis [22, 23], resulting in the apoptosis of tumor cells. The level of phospho-histone H2A.X and total p53 protein could be upregulated in cells by ruthenium(II) complexes [24], suggesting that apoptosis of tumor cells by triggering DNA damage-mediated p53 phosphorylation is the main mechanism of ruthenium(II) complexes. Preliminary studies by our research team have found that chiral ruthenium complexes can induce apoptosis of tumor cells by regulating the expression of Bcl-2 family protein [25]. Although the binding properties and toxicity of this type of ruthenium(II) complexes have been studied [26], little information was obtained on the binding behavior of chiral ruthenium complexes with *c-myc* G-quadruplex DNA and the effect on the expression of *c-myc*.

In this article, two chiral ruthenium(II) complexes, **Λ/Δ**-[Ru(bpy)$_2$(H_2iip)](ClO_4)$_2$ (**Λ-1** and **Δ-1**, bpy = 2,2-bipyridine; H_2ii*p* = 2-(indol-3-yl)imidazo[4,5*f*][1, 10]phenanthroline) (scheme 1), were designed to clarify the binding behavior of chiral ruthenium(II) complexes with *c-myc* G4 DNA. The results of the investigations show that both **Λ-1** and **Δ-1** can bind and stabilize the G-quadruplex conformation of *c-myc* with excellent binding affinity, and the activity of Taq polymerase and the growth of tumor cells were thus inhibited.

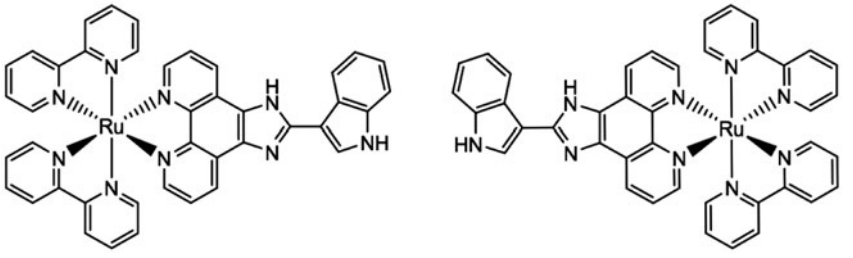

Scheme 1. The structures of the chiral ruthenium(II) complexes **Λ/Δ-1**.

2. Experimental

2.1. *Chemicals and methods*

All reagents and solvents were purchased commercially and used without purification unless noted. Distilled water was used in all experiments. Pu_{22} oligomers, the complementary guanine-rich strand 5′-TGAGGGTGGGTGGGTAA-3′, was purchased from Shanghai Gene-Pharma Co., Ltd. and formed G-quadruplex conformation as in the literature by renaturation for 24 h at 4 °C, after 90 °C, denaturation for 5 min. All aqueous solutions were prepared with double-distilled water. The Tris–HCl buffer consisting of Tris (10 mM) and KCl (100 mM), and the pH value was adjusted to 7.2 by HCl solution was applied to UV titration, fluorescence quenching, and circular dichroism (CD) spectra. $[Ru(bpy)_2Cl_2]\cdot 2H_2O$, $[Ru(py)_2(bpy)_2]$, $[Ru(bpy)_2(py)_2][O,O'$-dibenzoyl-D-tartrate$]\cdot 12H_2O$, and $[Ru(bpy)_2(py)_2]$ [*O*,*O*′-diben zoyl-L-tartrate]$\cdot 12H_2O$ were prepared and characterized according to the literature [27, 28].

2.2. *Physical measurements*

The ^{1}H NMR and ^{13}C NMR spectra were recorded in d^6-DMSO solution on a Bruker DRX 2500 spectrometer and electrospray ionization mass spectra (ESI-MS) were obtained in methanol on an Agilent 1100 ESI-MS system operating at room temperature. UV–vis absorption spectra and melting point were recorded on a Shimadzu UV-2550 spectrophotometer using 1-cm path length quartz cuvettes (3 mL). CD spectra were measured on a Jasco J-810 spectropolarimeter. ITC (isothermal titration calorimetry) experiments were carried out on an isothermal titration calorimeter (VP-ITC; MicroCal, Northampton, MA, USA) at 298.15 K with stirring at 394 rpm. Fluorescence melting curves were measured by a Roche Lightcycler 2.0 real-time PCR detection system. RT-qPCR assay was measured by PCR (biored IQ5).

The electronic absorption spectra were carried out at room temperature to determine the binding affinity between *c-myc* G4 DNA and the target complexes. Initially, 3.0 mL solutions of the ruthenium complexes were placed in the reference, and then the first spectrum was recorded from 200 to 700 nm. The titration processes were repeated until there was no change in the spectra for four titrations at least, indicating binding saturation had been achieved [26]. The intrinsic binding constants (K_b) for **1** and **2** with *c-myc* G4 DNA at IL absorption have been calculated following equations (1) and (2) according to the decay of IL absorption in the presence of *c-myc* G4 DNA.

$$(\varepsilon_a - \varepsilon_f)/(\varepsilon_b - \varepsilon_f) = [b - (b^2 - 2K^2C_t[\mathrm{DNA}]/\mathrm{S})]^{1/2}/2\mathrm{KC_t} \quad (1)$$

$$b = 1 + KC_t + K[DNA]/2S \quad (2)$$

CD spectra were measured on a Jasco J-810 spectropolarimeter. For each sample, at least three spectral scans were accumulated from 200 to 500 nm at room temperature in a 1.0 cm path length cell at a scanning rate of 50 nm/min.

FRET melting curves were measured by a Roche Lightcycler 2.0 real-time PCR detection system using a total reaction volume of 25 μL, 200 nM of labeled oligonucleotide and different concentrations of the ruthenium(II) complexes. Fluorescence readings with excitation at 470 nm and detection at 530 nm were taken at intervals of 1 °C from 37 to 95 °C.

The PCR stop assay were performed in 1 × PCR buffer containing 1 μL of each oligonucleotide, 5.5 μL dd H_2O, 12.5 μL Taq polymerase, and different concentrations of complexes. Reaction mixtures were incubated in a thermocycler with the following cycling conditions: 94 °C for 3 min, followed by 30 cycles of 94 °C for 30 s, 58 °C for 30 s, and 72 °C for 30 s.

The tested compounds were dissolved in DMSO with stock solution at 1 mM. Cell viability was determined by measuring the ability of cells to transform MTT to a purple formazan dye. Cells were seeded in 96-well cell culture platte (5×10^3 cells/well) for 48 h. The cells were then incubated with the tested compounds at different concentrations for 72 h. After incubation, 20 μL/well of MTT solution (5 mg/mL phosphate-buffered saline) was added and incubated for 5 h. The medium was aspirated and replaced with 150 μL/well DMSO to dissolve the formazan salt. The absorbance intensity, which reflects the cell growth condition, was measured at 570 nm using a microplate spectrophotometer (Versamax).

2.3. *Synthesis of H_2iip*

2-(1H-indol-3-yl)-1*H*-imidazo[4,5*f*][1, 10]phenanthroline (H_2iip) was synthesized according to the literature procedures [29] with some modification. A mixture of 1,10-phenanthroline-5,6-dione (0.315 g, 1.50 mM), 1H-indole-3-carbaldehyde (0.328 g, 1.5 mM), ammonium acetate (4.0 g, 51.9 mM), and glacial acetic acid (20 mL) was irradiated by microwave for 20 min at 100 °C. The reaction mixture was diluted with 40 mL water and then neutralized with aqueous ammonia. The crude products were filtered and washed with water, dried, and purified by 80–100-mesh silica gel filtration using ethanol as an eluent. Yield: 73.1%. ESI-MS (in DMSO, *m/z*): 334.4($[M - H]^-$), 370.0($[M + Cl]^-$), 704.9($[2\ M + Cl]^-$).

2.4. *Synthesis of Λ-[Ru(bpy)$_2$(H$_2$iip)](ClO$_4$)$_2$*

Λ-1 was synthesized following the literature procedure [27] but with some modifications. A mixture of **Λ**-[Ru(bpy)$_2$(py)$_2$][*O*,*O*′-dibenzoyl-L-tartrate]·12H_2O (170 mg, 0.3 mM), H_2iip (100 mg, 0.3 mM), and ethylene glycol (27 mL) was refluxed for 8 h under argon. The cooled reaction mixture was diluted with water. Adding sodium perchlorate to the filtered liquor gave an orange suspended solid. The dark red solid was collected and washed with small amounts of water and diethyl ether, then dried under vacuum, and purified by column chromatography on alumina. The solvent was removed under reduced pressure and red

microcrystals were obtained; yield: 63%. ESI-MS (in CH_3CN, *m/z*): 847.8 ($[M\text{-}ClO_4]^+$), 748.1 ($[M\text{-}2ClO_4 + H]^+$), 374.7 ($[M\text{-}2ClO_4]^{2+}$). UV–vis [λ (nm), ε ($M^{-1}\,cm^{-1}$) in 5% DMSO/H_2O]: 461.5 (13,000), 286.5 (66,200). CD[λ_{max}(nm), in 5% DMSO/H_2O, 10 μM]: +12.88. ^1H NMR (500 MHz, DMSO) δ 10.71 (d, J = 7.5 Hz, 2H, **7**), 10.54 (d, J = 8.1 Hz, 2H, **10**), 10.42 (d, J = 8.2 Hz, 2H, **6′** and **6**), 10.2 (d, J = 8.1 Hz, 2H, **α**), 9.82 (d, J = 2.8 Hz, 1H, **11**), 9.76 (t, J = 8.0 Hz, 2H, **4′**), 9.64 (t, J = 7.8 Hz, 2H, **4**), 9.60 – 9.55 (m, 2H, **β**), 9.46 (ddd, 2H, **9** and **8**), 9.39 (d, J = 5.5 Hz, 2H, **γ**), 9.17 (d, J = 5.5 Hz, 2H, **5′** and **3′**), 8.89 (ddd, 2H, **5**), 8.80 – 8.71 (s, 1H, **3**).

2.5. *Synthesis of Δ-[Ru(bpy)$_2$(H$_2$iip)](ClO$_4$)$_2$*

Δ-1 was prepared following the same procedure as above, but with **Δ**-$[Ru(bpy)_2(py)_2]$[*O*, *O′*-dibenzoyl-D-tartrate]•$12H_2O$ (170 mg, 0.3 mM); yield: 68%. ESI-MS (in CH_3CN, *m/z*): 847.9 ($[M\text{-}ClO_4]^+$), 748.3 ($[M\text{-}2ClO_4 + H]^+$), 374.9 ($[M\text{-}2ClO_4]^{2+}$). UV–vis [λ (nm), ε ($M^{-1}\,cm^{-1}$) in 5% DMSO/H_2O]: 461.0 (13,000), 286.5 (67,400). CD [λ_{max} (nm), in 5% DMSO/H_2O, 10 μM]: −12.83. ^1H NMR (500 MHz, DMSO) δ 10.71 (d, J = 8.2 Hz, 2H, **7**), 10.55 (d, 2H, **10**), 10.40 (dd, 4H, **6′** and **6**), 10.21 (d, J = 8.1 Hz, 2H, **α**), 9.97 (d, J = 2.8 Hz, 2H, **11**), 9.75 (t, J = 7.9 Hz, 2H, **4′**), 9.64 (t, J = 7.9 Hz, 2H, **4**), 9.60 – 9.56 (m, 2H, **β**), 9.55 (d, J = 4.3 Hz, 2H, **8** and **9**), 9.39 (d, J = 5.5 Hz, 2H, **γ**), 9.12 (tdd, 3H, **5′** and **3′**), 8.93 – 8.85 (m, 2H, **5**), 8.85 – 8.74 (m, 2H, **3**).

3. Results and discussion

3.1. *Synthesis and characterization*

The target complexes have been synthesized using chiral precursors and H_2iip, and precipitated using saturated perchlorate sodium solution. The obtained crude complexes were purified using column chromatography on alumina.

The ESI-MS of **Λ-1** exhibit a peak at *m/e* of 374.7 and the masses are 0.5 mass units apart (figure 1), indicating a dication. Thus, this ion peak can be attributed to $[M\text{-}2ClO_4]^{2+}$ (Calcd 374.9). The ion peak at *m/e* of 748.1 with a 1.0 mass unit separation [figure S2(a), see online supplemental material at http://dx.doi.org/10.1080/00958972.2015.1014352] is a monocation, and attributed to $[M\text{-}2ClO_4\text{-}H]^+$ (Calc. 748.0). The ion peak at *m/e* of 847.8 also gave a 1.0 unit apart [figure S2(b)], and can be attributed to $[M\text{-}ClO_4]^+$ (Calc. 848.0).

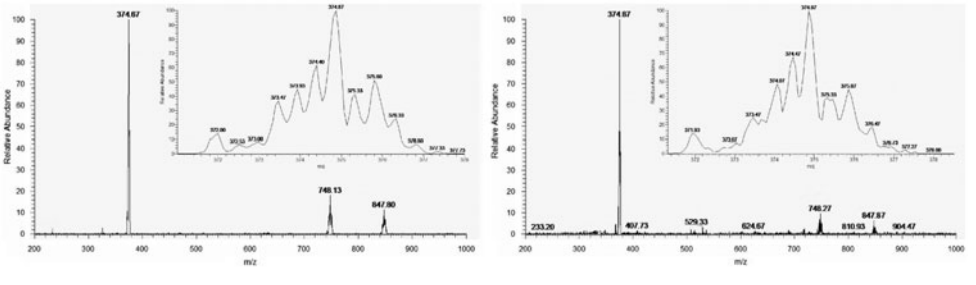

Figure 1. The ESI-MS spectra of **Λ-1** (left) and **Δ-1** (right).

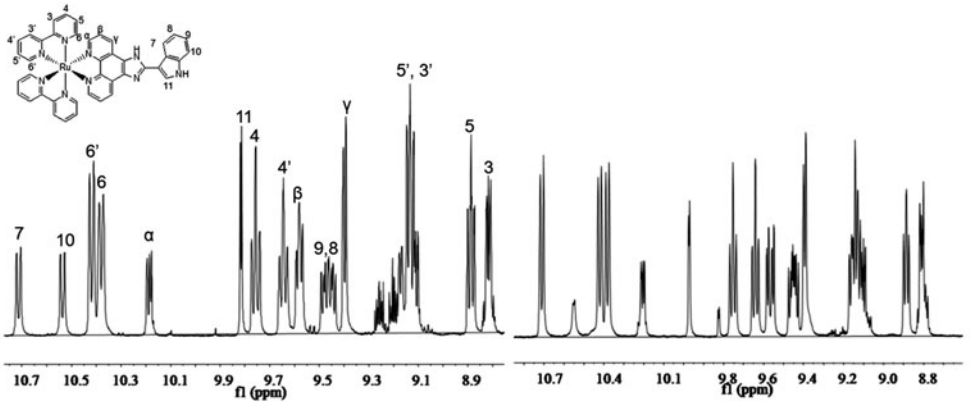

Figure 2. The ^{1}H NMR spectra of **Λ-1** (left) and **Δ-1** (right).

As for **Δ**-isomer, the ion peak at 374.7, 748.1, and 847.8 was also attributed to the corresponding $[M\text{-}2ClO_4]^{2+}$, $[M\text{-}2ClO_4\text{-}H]^{+}$, and $[M\text{-}ClO_4]^{+}$, respectively.

The chemical shifts of ^{1}H NMR spectrum for **Λ-1** attributed to the protons of H4′ and H4 in each bipyridyl ligand, appeared at 9.76 and 9.64 ppm, and H3′, H3 and H5′, H5 at 9.17, 8.80 and 8.89 ppm, respectively (figure 2). The chemical shift ascribe to H6′ and H6 appeared at 9.76 and 10.42 ppm, respectively. The proton resonace in the phenanthroline ring were appeared at chemical shift 10.2, 9.60–9.55 and 9.40 ppm, respectively. Besides, the chemical shift appeared at which attribute to 9.82, 9.46, 10.71 and 10.54 ppm can be ascribe to H11, H9 and H8, H7 and H10 in indole group, respectively. As for Δ-1, there were little difference at the chemical shift ascribe to H11 and H10 in indole group.

3.2. *The DNA-binding behavior of ruthenium(II) complexes with c-myc G4 DNA*

Small drugs stabilizing the conformation of *c-myc* G4 DNA can interface the expression of *c-myc* oncogene [25]. Thus, the binding behaviors of both isomers with *c-myc* G4 DNA have been investigated to clarify this.

3.2.1. Electronic titration. Electronic spectra are the most common methods to evaluate the interaction of transition metal complexes with biological macromolecules. In general ruthenium(II) complexes exhibit absorption in UV–vis spectroscopy, which will undergo hypochromism and red shift in the presence of biological molecules, and the degree of change depends on the binding affinity. The change of the electronic spectra for both **Λ-1** and **Δ-1** in the absence and in the presence of *c-myc* G4 DNA is illustrated in figure 3.

As shown in figure 3, the electronic spectra of **Λ-1** in Tris–HCl buffer (pH 7.2) solution exhibit the characteristic metal-to-ligand charge transfer (MLCT) absorption at 400–550 nm with maximum at 461 nm and the characteristic intraligand charge transfer (IL) absorption at 250–300 nm with maximum at 286 nm [30]. This was also observed for **Δ-1**, and the MLCT and IL absorptions appeared at 461 and 286 nm, respectively. As the concentration of *c-myc* G4 DNA is increased, the hypochromism in the IL band reaches 22.3%

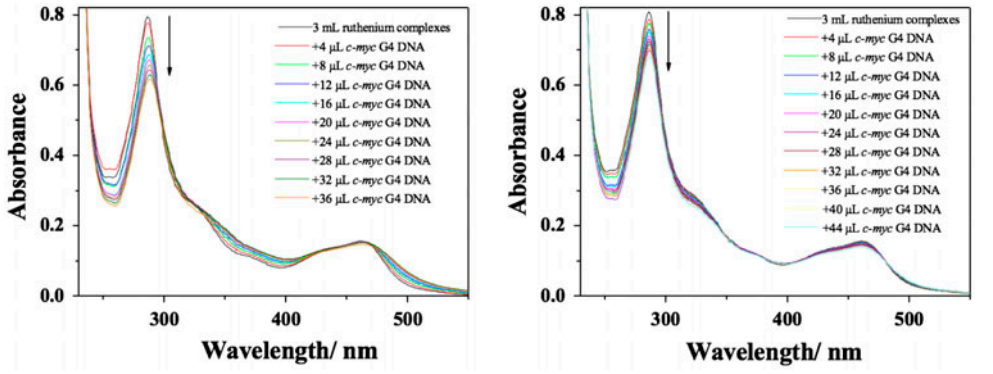

Figure 3. The electronic spectra of **Λ-1** (left) and **Δ-1** (right) in the absence and presence of *c-myc* G4 DNA. [Ru] = 10 μM, [DNA] = 100 μM. Arrow shows the absorbance changing upon increasing *c-myc* G4 DNA concentrations.

($\Delta\lambda$ = 2.0 nm) and 18.3% ($\Delta\lambda$ = 0.5 nm), respectively. Intrinsic binding constants (K_b) of 1.97 and 1.18 × 10^5 M^{-1} were obtained for **Λ-1** and **Δ-1**, respectively. The binding affinity of both isomers is comparable with that of $[Ru(L)(bpy)_2]ClO_4$ (L = (4-chloro-phenyl)-(1H-pyrrol-2-yl)-diazene and (4-nitro-phenyl)-(1H-pyrrol-2-yl)-diazene) [31, 32], and higher than that of $[RuX_2(PPh_3)L]$ (X = Cl, Br, L = 3-(benzothiazol-2-yliminomethyl)-naphthalen-2-ol) [33–35].

The binding of both isomers with *c-myc* G4 DNA has also been confirmed using ITC experiments and the results are listed in table 1.

ITC experiments were conducted at 298.15 K to afford the standard molar enthalpy change for binding (ΔH^0_m), the thermodynamics binding constant (K_b), and the binding stoichiometry (n), and the entropy was calculated by using the equation: $\Delta_b G^0_m = \Delta H^0_m - T\Delta_b S^0_m$ (Isothermal). The results show that both **Λ-1** and **Δ-1** bind with *c-myc* G4 DNA in a one-site mode and completely saturates at 1:1 stoichiometry; the standard binding constant calculated for **Λ-1** and **Δ-1** is 4.21 and 3.89 × 10^4 M^{-1}, respectively. These data suggested that the **Λ**-isomer binds with *c-myc* G4 DNA with subtle but detectable higher affinity than that of the **Δ**-isomer [36].

3.2.2. Circular dichroism spectra. The CD spectra offer useful information on the interaction of the small molecules with the biological macromolecules. To determine the formation of chiral ruthenium(II) complexes in the presence of *c-myc* G4 DNA, the CD spectra were employed as shown in figure 4.

A positive CD signal was observed at 250–300 nm with the maximum at 294 nm for isomer **Λ-1**, while a negative CD signal appeared at the same position for **Δ-1**. Upon addition

Table 1. Thermodynamic parameters for the binding of **Λ-1** and **Δ-1** to *c-myc* G4 DNA measured by ITC at 298.15 K.

Comp.	n (bases/comp)	$K_b \times 10^{-4}$ (M L^{-1})	$\Delta_b H^0_m$ (kcalM^{-1})	$\Delta_b G^0_m$ (kcalM^{-1})	$\Delta_b S^0_m$ (calM^{-1} K^{-1})
Λ-1	1	4.21	−8	−6.33	−5.6
Δ-1	1	3.89	−1.65	−24.1	−34.3

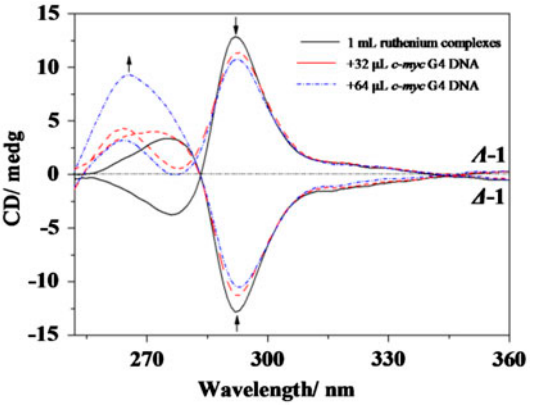

Figure 4. The CD spectra of **Λ-1** (upper) and **Δ-1** (lower) in the absence and presence of increasing amounts of *c-myc* G4 DNA. [Ru] = 10 μM, [DNA] = 100 μM.

of *c-myc* G4 DNA, the CD signal for both isomers decreased and the signal strengths for **Λ-1** and **Δ-1** decreased about 14.8 and 19.3%, respectively. The positive band at 265 nm appeared for **Δ-1**. These data suggest that the conformation of both isomers undergo disorder as *c-myc* G4 DNA was added to the solution [37, 38].

3.2.3. Fluorescence resonance energy transfer melting point curves. The FRET experiments have been conducted to investigate the thermodynamic stability of *c-myc* G-quadruplex DNA when treated with **Λ-1** and **Δ-1**; the results are illustrated in figure 5. The melting point obtained for *c-myc* G4 DNA is 44.0 °C. Upon addition of both isomers, the melting point of *c-myc* G4 DNA increased and is concentration dependent. At [Ru] = 3.0 μM, the Tm of *c-myc* G4 DNA in the presence of **Λ-1** and **Δ-1** increased to 53.5 (ΔT_m = 9.5 °C) and 52.3 °C (ΔT_m = 8.3 °C), respectively. These data indicate that both isomers enhance the thermodynamic stability of *c-myc* oligomer [39, 40]. These data are in agreement with those above, indicating that the **Λ**-isomer binds with *c-myc* G-quadruplex

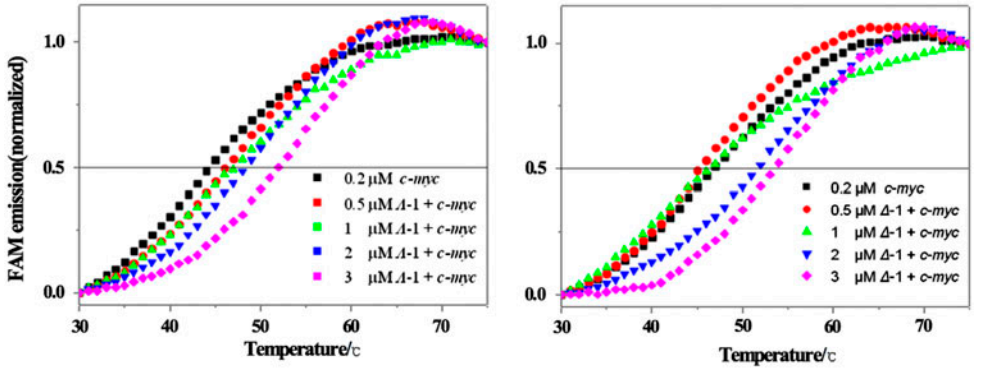

Figure 5. FRET melting profiles of 0.2 μM *c-myc* with **Λ-1** (left) and **Δ-1** (right).

DNA more tightly than does the **Δ**-isomer. This phenomenon was reported by Ji who observed a typical negative CD signal of the **Δ**-isomer in the racemic ruthenium(II) solution after equilibrium dialysis with double-strands calf-thymus DNA [41, 42]. These data also show that the structure of DNA molecules plays a key role in determining the DNA-binding behavior of chiral ruthenium(II) complexes.

3.3. *PCR-Stop assay*

The PCR-stop assay was utilized to evaluate the inhibitory activity of both **Λ-1** and **Δ-1** against Taq polymerase by stabilizing G-quadruplex conformation of the c-myc oligomer (figure 6). The PCR-stop assay has been conducted to determine whether these complexes inhibit the activity of Taq polymerase by stabilizing the G-quadruplex structure of the tested oligomer.

In the presence of G-quadruplex stabilizers, the template sequence was induced into a G-quadruplex structure that blocked hybridization and detection of the final PCR product [43]. As shown in figure 6, the single strand *c-myc* G4 DNA will hybridize with a complementary strand in the presence of Taq polymerase (Control). When the ruthenium(II) complexes **Λ-1** or **Δ-1** were added to the solution, replication of *c-myc* oligomer was suppressed, which is attributed to the G-quadruplex structure induced to block the hybridization with a complementary strand [44].

3.4. *Biological activity*

The *in vitro* inhibitory activities of both isomers against human breast cells (MDA-MB-231, MCF-7), human esophageal carcinoma cells (EC-1), human hepatocellular liver carcinoma

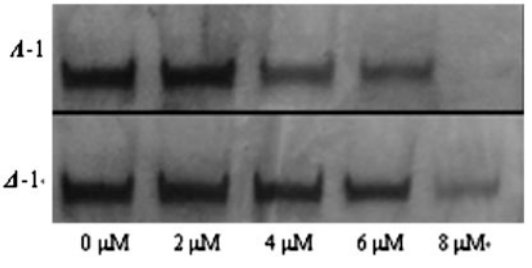

Figure 6. The effect of both isomers **Λ-1** (up) and **Δ-1** (down) on the hybridization of Taq polymerase. [Ru]=0-8 μM.

Table 2. The inhibitory activity (IC_{50}/μM) of both isomers and cisplatin against selected cell lines.

	Inhibitory activity/IC_{50}				
Comp.	MDA-MB-231	MCF-7	EC-1	HepG2	HaCat
Λ-1	82.1 ± 1.2	158.3 ± 1.8	148.0 ± 2.6	135.7 ± 1.0	120.7 ± 1.0
Δ-1	46.5 ± 1.6	176.2 ± 3.5	173.4 ± 1.0	193.9 ± 0.8	33.3 ± 0.5
Cisplatin	36.1 ± 0.8	42.3 ± 1.9	/	7.23 ± 2.4	7.48 ± 1.3

cells (HepG2), and normal cuticle cells (HaCat) were evaluated by the MTT assay after 48 h of treatment, and the results are listed in table 2.

As shown in table 2, both **Λ-1** and **Δ-1** exhibit acceptable inhibitory activity toward breast cancer cells. The IC_{50} values determined for **Δ-1** (46.5 μM), which was cytotoxicity toward MDA-MB-231 cells in this study, is close to cisplatin at the same conditions (IC_{50} = 36.1 μM). Moreover, both isomers were less cytotoxic than cisplatin on the immortal human keratinocyte cell line (HaCat) studied in this work, suggestive of a better therapeutic profile than cisplatin (IC_{50} = 7.5 μM). These data indicate that those ruthenium (II) complexes have potential utility in clinical studies with acceptable inhibitory activity against tumor cells but low toxicity [25].

Generally speaking, the more binding capacity of ruthenium(II) complexes with DNA, the more bioactivity will exist. However, binding behavior is just one aspect; those complexes get the dense region of DNA in the nucleus *in vitro.* In fact, ruthenium(II) complexes bearing different ligands often show different distribution coefficients. Recent studies conducted by Gasser show that ruthenium(II) complexes exert their inhibitory activity through a mitochondria-related pathway, like cisplatin, rather than *via* interaction with nuclear DNA [45]. Therefore besides the DNA binding other factors, for example, uptake levels of ruthenium(II) complexes by cancer cells [46], should be considered when choosing a candidate with high activity, and more detailed investigations on the chemical biology and pharmacology of these compounds are now underway.

4. Conclusion

Two chiral ruthenium(II) complexes, **Λ/Δ**-[Ru(bpy)$_2$(H_2iip)](ClO_4)$_2$ (**Λ-1** and **Δ-1**), were synthesized and characterized by ESI-MS, ^{1}H NMR, and CD spectra. Studies on the interaction of both isomers with *c-myc* G4 DNA show that both isomers can bind and stabilize the *c-myc* G-quadruplex DNA, with the **Λ**-isomer exhibiting a subtle but detectable higher binding affinity than that of the **Δ**-isomer. Both isomers can inhibit the growth of tumor cells. These chiral ruthenium(II) complexes can be developed as potential inhibitors by targeting *c-myc* G-quadruplex DNA in chemotherapy.

Acknowledgements

The author wishes to express sincere appreciation and gratitude to Professor. Jiao Guo in Guandong Pharmaceutical University for her kind assistance and guidance and MS. Xiao-Jun Liang for her support in the preparation of this dissertation.

Funding

This work was supported by the Science and Technology Item Foundation of Guangzhou [grant number 2011J5200017], [grant number 2013J4100072]; the Joint Natural Sciences Fund of the Department of Science and Technology & the First Affiliated Hospital of Guangdong Pharmaceutical University [grant number GYFYLH201309].

References

[1] G.L. Duveneck, C.V. Kumar, N.J. Turro, J.K. Barton. *J. Phys. Chem.*, **92**, 2028 (1988).
[2] S. Delaney, M. Pascaly, P.K. Bhattacharya, K. Han, J.K. Barton. *Inorg. Chem.*, **41**, 1966 (2002).
[3] X. Liang, S. Suwanrumpha, R.B. Freas. *Inorg. Chem.*, **30**, 652 (1991).
[4] S. Dhar, A.R. Chakravarty. *Inorg. Chem.*, **44**, 2582 (2005).
[5] E. Paleček, M. Bartošík. *Chem. Rev.*, **112**, 3427 (2012).
[6] J. Collins, J. Aldrich-Wright, R. Rixon. *Inorg. Chem.*, **39**, 4377 (2000).
[7] G. Ruchi, M. Lallan. *Inorg. Chem.*, **51**, 3057 (2012).
[8] J. Wang, Y. Chen, J. Ren, C. Zhao, X. Qu. *Nucleic Acids Res.*, **42**, 1 (2014).
[9] F. Gao, H. Chao, F. Zhou, L. Xu, K. Zheng, L.N. Ji. *Helv. Chim. Acta*, **90**, 36 (2007).
[10] S.K. Singh, S. Joshi, A.R. Singh, J.K. Saxena, D.S. Pandey. *Inorg. Chem.*, **46**, 10869 (2007).
[11] X. Chen, J.H. Wu, Y.W. Lai, R. Zhao, H. Chao, L.N. Ji. *Dalton Trans.*, **42**, 4386 (2013).
[12] P. Zhao, J. Li, L.J. Yang, J.Z. Lu, H.M. Guo, L.N. Ma, B.H. Ou. *J. Coord. Chem.*, **66**, 4220 (2013).
[13] W.J. Mei, X.Y. Wei, Y.J. Liu, B. Wang. *Transition Met. Chem.*, **33**, 907 (2008).
[14] C. Rajput, R. Rutkaite, L. Swanson, I. Haq, J.A. Thomas. *Chem. Eur. J.*, **12**, 4611 (2006).
[15] Z. Zhang, Q. Wu, X.H. Wu, F.Y. Sun, L.M. Chen, J.C. Chen, S.L. Yang, W.J. Mei. *Eur. J. Med. Chem.*, **80**, 316 (2014).
[16] K. Kelly, B.H. Cochran, C.D. Stiles, P. Leder. *Cell*, **35**, 603 (1983).
[17] H. Shim, C. Dolde, B.C. Lewis, C.S. Wu, G. Dang, R.A. Jungmann, R. Dalla-Favera, C.V. Dang. *Proc. Natl. Acad. Sci. USA*, **94**, 6658 (1997).
[18] S. Pelengaris, M. Khan, G. Evan. *Nat. Rev. Cancer*, **2**, 764 (2002).
[19] G.I. Evan, A.H. Wyllie, C.S. Gilbert, T.D. Littlewood, H. Land, M. Brooks, C.M. Waters, L.Z. Penn, D.C. Hancock. *Cell*, **69**, 119 (1992).
[20] S.M. Zhu, H.L. Wu, F.T. Wu, D.T. Nie, S.J. Sheng, Y.Y. Mo. *Cell Res.*, **18**, 350 (2008).
[21] C.V. Dang, L.M. Resar, E. Emison, S. Kim, Q. Li, J.E. Prescott, D. Wonsey, K. Zeller. *Exp. Cell Res.*, **253**, 63 (1999).
[22] T.A. Brooks, L.H. Hurley. *Genes Cancer*, **1**, 641 (2010).
[23] M.J. Morris, K.L. Wingate, J. Silwal, T.C. Leeper, S. Basu. *Nucleic Acids Res.*, **40**, 4137 (2012).
[24] L.L. Li, W.Q. Cao, W.J. Zheng, C.D. Fan, T.F. Chen. *Dalton Trans.*, **41**, 12766 (2012).
[25] T.F. Chen, W.J. Mei, Y.S. Wong, J. Liu, Y. Liu, H.S. Xie, W.J. Zheng. *MedChemComm*, **1**, 73 (2010).
[26] J. Liu, L.F. Tan, L.H. Jin, F. Luan. *DNA Cell Biol.*, **31**, 250 (2012).
[27] W.J. Mei, J. Liu, K. Zheng, L. Lin, H. Chao, A. Li, F. Yun, L.N. Ji. *Dalton Trans.*, **7**, 1352 (2003).
[28] W.J. Mei, Y.X. Liu, L.J. Lin, K.C. Zheng, L.N. Ji. *Transition Met. Chem.*, **30**, 82 (2005).
[29] Z. Zhang, Q. Wang, Q. Wu, X.Y. Hu, W.J. Mei, W.L. Wu, W.J. Zheng. *Chem. J. Chin. Univ.*, **33**, 2441 (2012).
[30] G. Achilleas, M. Gerasimos, H. Nick. *Eur. J. Med. Chem.*, **16**, 3326 (2004).
[31] H. Paul, T. Mukherjee, M. Mukherjee, T.K. Mondal, A. Moirangthem, A. Basu, E. Zangrando, P. Chattopadhyay. *J. Coord. Chem.*, **66**, 2747 (2013).
[32] J. Wang, X. Zhao, F. Yan, L. Wei, Q. Pan, F. Zhang, P. Yang. *J. Coord. Chem.*, **66**, 3848 (2013).
[33] S. Sathiyaraj, R.J. Butcher, C. Jayabalakrishnan. *J. Coord. Chem.*, **66**, 580 (2013).
[34] M. Shilpa, C. Shobha Devi, P. Nagababu, J. Naveena Lavanya Latha, R. Pallela, V. Rao Janapala, K. Aravind, S. Satvanaravana. *J. Coord. Chem.*, **66**, 1661 (2013).
[35] J. Jaumot, R. Gargallo. *Curr. Pharm. Des.*, **18**, 1900 (2012).
[36] C.B. Spillane, M.N.V. Dabo, N.C. Fletcher, J.L. Morgan, F.R. Keene, I. Haq, N.J. Buurma. *J. Inorg. Biochem.*, **102**, 673 (2008).
[37] J. Sun, Y. An, L. Zhang, H.Y. Chen, Y. Han, Y.J. Wang, Z.W. Mao, L.N. Ji. *J. Inorg. Biochem.*, **105**, 149 (2011).
[38] D. Sun, B. Thompson, B.E. Cathers, M. Salazar, S.M. Kerwin, J.O. Trent, T.C. Jenkins, S. Neidle, L.H. Hurley. *J. Med. Chem.*, **40**, 2113 (1997).
[39] X. Chen, J.H. Wu, Y.W. Lai, R. Zhao, H. Chao, L.N. Ji. *Dalton Trans.*, **42**, 4386 (2013).
[40] L.Y. Li, H.N. Jia, H.J. Yu, K.J. Du, Q.T. Lin, K.Q. Qiu, H. Chao, L.N. Ji. *J. Inorg. Biochem.*, **113**, 31 (2012).
[41] J.G. Liu, B.H. Ye, Q.L. Zhang, X.H. Zou, Q.X. Zhen, X. Tian, L.N. Ji. *J. Biol. Inorg. Chem.*, **5**, 119 (2000).
[42] W.J. Mei, J. Liu, K.C. Zheng, L.J. Lin, H. Chao, A.X. Li, F.C. Yun, L.N. Ji. *J. C. S. Dalton Trans.*, **7**, 1352 (2003).
[43] D. Sun, L.H. Hurley. *Methods Mol. Biol.*, **608**, 65 (2010).
[44] T. Lemarteleur, D. Gomez, R. Paterski, E. Mandine, P. Mailliet, J.-F. Riou. *Biochem. Biophys. Res. Commun.*, **323**, 802 (2004).
[45] V. Pierroz, T. Joshi, A. Leonidova, C. Mari, J. Schur, I. Ott, L. Spiccia, S. Ferrari, G. Gasser. *J. Am. Chem. Soc.*, **134**, 20376 (2012).
[46] M.R. Gill, J.A. Thomas. *Chem. Soc. Rev.*, **41**, 3179 (2012).